MOLECULAR AND CELLULAR BIOLOGY, Mar. 2002, p. 1858–1867 Vol. 22, No. 6
0270-7306/02/$04.00+0 DOI: 10.1128/MCB.22.6.1858–1867.2002

The Rab27a/Granuphilin Complex Regulates the Exocytosis of Insulin-Containing Dense-Core Granules

Zhaohong Yi,[1] Hiromi Yokota,[1] Seiji Torii,[1] Takeo Aoki,[2] Masahiro Hosaka,[1] Shengli Zhao,[1] Kuniaki Takata,[2] Toshiyuki Takeuchi,[1] and Tetsuro Izumi[1]*

Department of Molecular Medicine, Institute for Molecular and Cellular Regulation, Gunma University, Maebashi, Gunma 371-8512,[1] and Department of Anatomy and Cell Biology, Gunma University School of Medicine, Maebashi, Gunma 371-8511,[2] Japan

Received 27 April 2001/Returned for modification 26 June 2001/Accepted 30 November 2001

Recently, we identified and characterized a novel protein, granuphilin, whose domain structure is similar to that of the Rab3 effector protein rabphilin3 (J. Wang, T. Takeuchi, H. Yokota, and T. Izumi, J. Biol. Chem. 274:28542–28548, 1999). Screening its possible Rab partner by a yeast two-hybrid system revealed that an amino-terminal zinc-finger domain of granuphilin interacts with Rab27a. Granuphilin preferentially bound to the GTP form of Rab27a. Formation of the Rab27a/granuphilin complex was readily detected in the pancreatic beta cell line MIN6. Moreover, the tissue distributions of Rab27a and granuphilin are remarkably similar: both had significant and specific expression in pancreatic islets and in pituitary tissue, but no expression was noted in the brain. Analyses by immunofluorescence, immunoelectron microscopy, and sucrose density gradient subcellular fractionation showed that Rab27a and granuphilin are localized on the membrane of insulin granules. These findings suggest that granuphilin functions as a Rab27a effector protein in beta cells. Overexpression of wild-type Rab27a and its GTPase-deficient mutant significantly enhanced high K^+-induced insulin secretion without affecting basal insulin release. Although Rab3a, another exocytotic Rab protein, has some similarities with Rab27a in primary sequence, intracellular distribution, and affinity toward granuphilin, overexpression of Rab3a caused different effects on insulin secretion. These results indicate that Rab27a is involved in the regulated exocytosis of conventional dense-core granules possibly through the interaction with granuphilin, in addition to its recently identified role in lysosome-related organelles.

The protein families that mediate vesicle trafficking are conserved through phylogeny from yeast to humans, as well as throughout the cell from the endoplasmic reticulum to the plasma membrane (4). The membrane fusion reaction requires integral membrane proteins termed soluble *N*-ethylmaleimide-sensitive factor attachment protein receptors (SNAREs). SNAREs function through the association of their cytoplasmic domains to form coiled coils. The Rab family of low-molecular-weight GTPases is also believed to regulate the processes of membrane targeting and fusion (30). Rab proteins are molecular switches that cycle between a GTP- and membrane-bound, active state and a GDP-bound, cytosolic, inactive state. These two forms of Rab are converted from one to the other by the action of GDP/GTP exchange factor and GTPase-activating protein. Active GTP-bound Rab is thought to function by binding to effector proteins associated with specific membrane components. In several systems, Rab proteins and their effectors have been shown to mediate a SNARE-independent initial association of membranes, termed tethering, which is the first step of the docking stage. Furthermore, subsequent trans-SNARE pairing may also be regulated by Rab proteins and their effectors. For example, a complex of Rab5 and the endosome-tethering protein EEA1 regulates endosome fusion by oligomerizing with syntaxin 13, a component of the SNARE machinery (24).

Each vesicle-trafficking step involves a set of different members of the Rab and SNARE protein families localized to distinct membrane compartments. Among these trafficking routes, multicellular organisms have developed a highly regulated exocytosis mechanism that occurs only in response to an intracellular Ca^{2+} signal generated by secretagogues. These secretory cells contain the special vesicles to store and release secretory products. Recent progress in biochemical studies of synaptic vesicles at nerve termini has revealed a number of molecules possibly involved in these processes. To date, Rab3 and its putative effector proteins, rabphilin3 and RIM, are the best candidates for exocytotic Rab and Rab effectors in neurons (20). Although large dense-core granules, another type of secretory vesicles in endocrine and exocrine cells, have been less well characterized biochemically due to their low abundance, recent evidence suggests that Rab3 also functions in endocrine cells such as adrenal chromaffin cells (18) and pancreatic beta cells (32). rabphilin3, however, is not expressed in pancreatic beta cells (32), whereas it is specifically expressed in brain and adrenal gland tissues and is associated with synaptic vesicles at nerve termini. Thus, it is conceivable that any Rab and/or effector proteins may act as regulators for insulin secretion. Recently, we identified a novel rabphilin3-like protein, granuphilin, in pancreatic beta cells (37). Similar to rabphilin3, this protein contains an amino-terminal zinc-finger motif and carboxyl-terminal C_2 domains. Granuphilin, however, differs from rabphilin3 in a number of ways, including tissue distribution and subcellular localization (37). Granuphilin is expressed

* Corresponding author. Mailing address: Department of Molecular Medicine, Institute for Molecular and Cellular Regulation, Gunma University, 3-39-15 Showa-machi, Maebashi, Gunma 371-8512, Japan. Phone: 81-27-220-8856. Fax: 81-27-220-8860. E-mail: tizumi@showa.gunma-u.ac.jp.

in pancreatic beta cells and pituitary tissue but is not significantly expressed in other major organs such as the brain. It is associated with dense-core granules but not with synaptic-like microvesicles in pancreatic beta cells. The unique distribution pattern of granuphilin suggests that it may be involved in the regulated exocytosis of dense-core granules in these endocrine tissues. In the present study, we report that Rab27a interacts with granuphilin in beta cells. In addition, Rab27a and granuphilin show remarkably similar tissue and subcellular distributions. Moreover, overexpression of Rab27a in beta cell lines significantly enhances high K^+-induced insulin secretion. Identification of a novel complex, Rab27a/granuphilin, should help elucidate the mechanism of regulated exocytosis in endocrine cells, which thus far has been poorly characterized.

MATERIALS AND METHODS

Construction of a MIN6 cDNA fusion library. Poly(A)$^+$ RNA was prepared from total RNA of MIN6 cells by using oligo(dT)-cellulose spun columns as described previously (15). First-strand cDNA was synthesized at 42°C from 3.2 μg of poly(A)$^+$ RNA in 50 μl of reaction buffer with 16 nmol of a random nonamer (TaKaRa Biomedicals, Kusatsu, Japan) and 1,600 U of Superscript II reverse transcriptase (GIBCO/BRL, Rockville, Md.). This ratio of primer to template ensured the enrichment of synthesized cDNAs 400 to 1,000 nucleotides in length. Second-strand synthesis was carried out with *Escherichia coli* DNA polymerase I (400 U/ml), *E. coli* DNA ligase (100 U/ml), and RNase H (22 U/ml). The ends of the resultant cDNA were blunted with T4 DNA polymerase. The cDNA (2.4 μg) was then ligated with an *Eco*RI (*Not*I) adapter (7 μg; 5′-P-GTCGACGCGGCCGCG-3′ and 5′-OH-AATTCGCGGCCGCGTCGAC-3′). After digestion with *Not*I for 4 h, cDNA (>400 nucleotides in length) was purified by column chromatography using SizeSep 400 spun columns (Amersham Pharmacia Biotech, Little Chalfont, Buckinghamshire, United Kingdom). The cDNA (700 ng) was then ligated into pVP16 (100 ng; *Not*I dephosphorylated) (17). *E. coli* strain DH10B was transformed with this cDNA by electroporation, and the amplified cDNA library was purified and used for yeast two-hybrid screening.

Yeast two-hybrid screening. The N-terminal domain containing a zinc-finger motif of granuphilin was amplified by PCR with primers 5′-CGGAATTCCTA GACCTCTCTTTTCTGTC-3′ and 5′-GAGTCGACCCATCTGTGTCTGCTG AA-3′, digested with *Eco*RI and *Sal*I, and then inserted into pBTM116 (2). This construct (pLexGrp.zf) encodes amino acids 5 to 163 of granuphilin fused to LexA. The C-terminal domain containing two C_2 domains, corresponding to amino acids 315 to 673 of granuphilin-a, was similarly amplified with primers 5′-CCGAATTCATTGACCACCTGGTGAAGT-3′ and 5′-ATGTCGACTCAT ACACCCAGCTTCTG-3′ and subcloned into pBTM116 (pLexGrp.C_2AB). Transformation of yeast strain L40 was performed as described previously (17). Briefly, a 1-liter culture of L40, containing a bait plasmid, was transformed with 500 μg of the MIN6 cDNA fusion library and 10 mg of denatured salmon sperm carrier DNA by the lithium acetate method with dimethyl sulfoxide addition (10% final concentration). After 4 h of recovery in 1 liter of synthetic complete medium (Trp$^-$ Leu$^-$ Ura$^-$), the transformants were plated onto medium to select for histidine prototrophy (Trp$^-$ Leu$^-$ Ura$^-$ His$^-$ Lys$^-$) with the addition of 5 mM 3-aminotriazole. Histidine-positive clones were lysed in liquid nitrogen and assayed for β-galactosidase (β-Gal) activity on filters. Positive library plasmid DNA was prepared as described previously (16) and isolated by transformation into *E. coli* HB101 and by selection for leucine prototrophy on minimal plates. For liquid β-Gal assays, bait and prey vectors were cotransformed into yeast and plated on Trp$^-$ Leu$^-$ Ura$^-$ plates. Single colonies were grown in liquid culture for 40 h before collection, and the β-Gal activity and protein content of each culture were determined as described previously (2).

Molecular cloning of Rab27a and Rab3a cDNA and construction of site-directed mutagenesis. The Rab27a cDNA isolated by two-hybrid interaction was radiolabeled by random priming and used to screen a βHC9/MIN6 cell cDNA library (15). Mouse Rab3a cDNA was isolated by reverse transcription-PCR from total RNA of MIN6 cells as described previously (15), using the primers designed from the mouse Rab3a sequence previously reported (3). Site-directed mutagenesis of Rab27a and Rab3a was performed using the double PCR strategy as described previously (15). The primers used are as follows: 5′-CTGGATCC TGTCGGATGGAGATTACGA-3′ and 5′-CTGAATTCTCTCAACAGCCAC ACAACC-3′ for Rab27a, 5′-TTATGGGACACGGCGGGGCTGGAGAGGTT TCGTAGCTTAA-3′ and 5′-CCCCGCCGTGTCCCATAACT-3′ for Rab27a Q78L, 5′-GACTCTGGGGTAGGGAAGAACAGTGTACTCTACCAGTAC A-3′ and 5′-CTTCCCTACCCCAGAGTCTC-3′ for Rab27a T23N, 5′-ATAGT GCTGTGTGGAATTAAGAGTGA-3′ and 5′-TTCCAGGTCACTCTTAATT CCACACA-3′ for Rab27a N133I, 5′-CTGGATCCTGGCTTCCGCCACAGAC TCT-3′ and 5′-CTGAATTCGCTCAGCAGGCACAATCCTGA-3′ for Rab3a, 5′-ATCTGGGACACAGCAGGGCTAGAGCGGTACCGCACCATCA-3′ and 5′-CCCTGCTGTGTCCCAGATCT-3′ for Rab3a Q81L, 5′-GAACAGCAGCG TGGGCAAAAACTCGTTCCTCTTCCGCTA-3′ and 5′-TTTTGCCCACGCT GCTGTTC-3′ for Rab3a T36N, and 5′-GTGCTGCTGGTGGGAATCAAGTG TGA-3′ and 5′-TCCATGTCACACTTGATTCCCACC-3′ for Rab3a N135I. The amplified PCR products were digested by *Bam*HI and *Eco*RI and subcloned into pVP16. The insert of each construct was directly sequenced. These Rab and granuphilin cDNAs were subcloned into pcDNA3.1/HisC (Invitrogen, Carlsbad, Calif.), pcDNA3/HA (36), and pGEX4T-1 (Amersham Pharmacia Biotech), which add the Xpress epitope tag, triple hemagglutinin (HA) epitope tag, and glutathione *S*-transferase (GST) tag at the N terminus of the cloned cDNA, respectively.

Antibodies. Rabbit antibodies against the carboxyl-terminal granuphilin-a peptide (αGrp-aC) have been described previously (37). Rabbit antigranuphilin antibodies (αGrp-N) were also produced against a peptide corresponding to amino acids 205 to 220 of granuphilin, CSYTADSDSTSRRDSLD, and recognize both granuphilin-a and granuphilin-b. Mouse monoclonal antibodies against Rab27a and Rab3a were purchased from Transduction Laboratories (Lexington, Ky.). Rabbit anti-Rab27a antibodies against GST-fused mouse Rab27a protein were also produced and used for immunoelectron microscopy. Antisynaptophysin mouse, anti-Xpress mouse, and anti-HA rat monoclonal antibodies were purchased from Progen Biotechnik (Heidelberg, Germany), Invitrogen, and Roche Diagnostics (Mannheim, Germany), respectively. Guinea pig anti-porcine insulin serum was a gift from K. Wakabayashi and H. Kobayashi (Gunma University). Immunoreactive insulin was measured as described previously (37). Immunoblotting and immunoprecipitation were performed as described previously (15).

Immunostaining and confocal microscopy. MIN6 cells on eight-well Lab-Tek chamber slides (Nunc, Naperville, Ill.) were fixed in 4% paraformaldehyde and 3% sucrose in 0.1 M phosphate buffer, pH 7.4, for 30 min at 4°C. After treatment with 50 mM NH_4Cl in phosphate buffer for 20 min to quench aldehyde groups, the cells were made permeable by treatment with phosphate buffer containing 0.5 M NaCl, 0.1% polyoxyethylene sorbitan monolaurate, and 0.1% Triton X-100 for 21 min at room temperature. Samples were blocked with 2% normal donkey serum, incubated overnight at 4°C with primary antibodies, and further incubated for 2 h at room temperature with corresponding rhodamine Red-X- or fluorescein isothiocyanate-conjugated, species-specific anti-immunoglobulin G secondary antibodies (Jackson ImmunoResearch, West Grove, Pa.). The specimens were observed with an Axioplan 2 fluorescence microscope (Carl Zeiss, Oberkochen, Germany) equipped with a laser confocal system (MRC-1024; Bio-Rad Laboratories, Hercules, Calif.). Plan-Apochromat objectives of ×63 (numerical aperture 1.4) and ×100 (numerical aperture 1.4) (Carl Zeiss) were used. Some specimens were observed with an epifluorescence microscope (BX-50: Olympus Optical Co., Tokyo, Japan). Images were captured and processed with Bio-Rad LaserSharp software and processed using Adobe Photoshop software.

Immunoelectron microscopy. Mice were perfused for 15 min with 0.05% glutaraldehyde–4% paraformaldehyde in 0.1 M phosphate buffer, pH 7.4. The pancreata were excised, cut into small pieces, and immersed for 30 min at 4°C in 4% paraformaldehyde in 0.1 M phosphate buffer (pH 7.4) containing 3% sucrose. They were then infiltrated with 2.3 M sucrose and rapidly frozen in liquid nitrogen. Ultrathin frozen sections were cut with a Reichert Ultracut S (Reichert-Jung, Vienna, Austria) equipped with an FCS cryosectioning system and incubated with primary antibodies and then 5-nm or 10-nm colloidal gold-conjugated secondary antibodies (Amersham Pharmacia Biotech). The specimens were embedded in a mixture of 2% methylcellulose and 0.4% uranyl acetate (12). They were observed with a JEOL JEM-100CX electron microscope (Tokyo, Japan). To see the distribution of Rab27a and granuphilin in pancreatic beta cells, electron micrographs were randomly taken in the immunolabeled sections over the cytoplasm at a magnification of ×18,000. Numbers of colloidal gold particles associated with secretory granules were counted in each micrograph. Gold particles as close as 60 nm to the granule membrane were considered to be granule associated.

Linear sucrose density gradients and cell fractionation. A linear sucrose density gradient (15 to 70% [wt/vol]) buffered with a solution containing 4 mM HEPES (pH 7.4) and 1.5 mM EDTA was formed by tilt tube rotation using a Gradient Master (BioComp Instruments, Fredericton, Canada) (9) for 15 min at

70° and 6 rpm, followed by 6 min at 58° and 9 rpm. MIN6 cells (two 10-cm plates) were detached from the dishes by a 20-min incubation in phosphate-buffered saline containing 10 mM EDTA at 37°C, pelleted by centrifugation, and homogenized in buffer containing 250 mM sucrose, 4 mM HEPES (pH 7.4), 1 mM $MgCl_2$, 0.005% DNase, and the following protease inhibitors: 1 mM phenylmethylsulfonyl fluoride and 10 μg (each) of aprotinin, pepstatin A, and leupeptin per ml. The homogenate was centrifuged at 5,000 × *g* for 10 min at 4°C. The resultant supernatant with the addition of 1.5 mM EDTA was layered onto the gradient and was centrifuged at 30,000 rpm for 18 h at 4°C in an RPS40T rotor (Hitachi Koki, Katsuta, Japan). Gradients were fractionated by piston displacement from the top down (8) using the BioComp Piston Gradient Fractionator. Samples for gel analysis were precipitated directly from gradient fractions by adding trichloroacetic acid to 10% (wt/vol) and bovine serum albumin to 0.01%, chilling for 15 min, and pelleting for 10 min at 10,000 × *g* in a microcentrifuge. Pellets were then washed twice with acetone and analyzed by immunoblotting.

Preparation of recombinant adenovirus and measurement of insulin secretion. The cDNAs of wild-type and mutant Rab27a and Rab3a with the Xpress epitope tag at the N terminus were inserted into the *Swa*I site of pAxCAwt (TaKaRa Biomedicals), which contains the CAG promoter. The ligation mixture was packaged in vitro using Gigapack III XL packaging extract (Stratagene, La Jolla, Calif.). Recombinant adenoviruses were generated in human embryonic kidney 293 cells as described previously (26). AxCALacZ, which expresses bacterial β-Gal, was used as a control adenovirus. MIN6 cells were seeded at 10^6 cells in 12-well dishes (2.5-cm plates). On the next day, the cells were infected with recombinant adenoviruses 40 h before experiments. The cells were incubated for 2 h in modified Krebs-Ringer buffer (120 mM NaCl, 5 mM KCl, 24 mM $NaHCO_3$, 1 mM $MgCl_2$, 2 mM $CaCl_2$, 15 mM HEPES [pH 7.4], 0.1% bovine serum albumin, 2 mM glucose) and then were incubated for 30 min in the same buffer or the buffer modified to include high K^+ (60 mM KCl–65 mM NaCl). Insulin in the medium was measured.

Nucleotide sequence accession number. For the sequence of the full-length mouse Rab27a cDNA, the DDBJ-GenBank-EBI accession number is AB046693.

RESULTS

Identification of the Rab proteins that interact with granuphilin. Granuphilin has a domain structure similar to that of rabphilin3, an effector protein of Rab3, and is thus expected to interact with some Rab proteins. Molecules that bind to the N-terminal zinc-finger domain of granuphilin were screened from a MIN6 cell cDNA library by the yeast two-hybrid system. One of the cDNAs encodes a protein whose amino acid sequence is homologous to that of rat Rab27a. This clone spanned nearly the entire coding region of Rab27a, omitting the C-terminal cysteine residue. The sequence of a full-length mouse Rab27a cDNA was determined. Among Rab sequences, Rab27a has the highest homology with members of the Rab3 subfamily (40% similarity on the amino acid level); one exception, however, is Rab27b (72% similarity), which was recently isolated and identified as another Rab27 isoform (7). Rab27a lacks a region corresponding to the N-terminal 13- to 21-amino-acid extension of Rab3 isoforms but has a unique 9-amino-acid insertion at residues 55 to 63. Because Rab3 is generally thought to be involved in regulated exocytosis and possibly forms a complex with granuphilin, the interactions of granuphilin with Rab27a and Rab3a were compared by using yeast two-hybrid assays (Table 1). Mutant forms of these Rab proteins were also constructed based on well-characterized mutations described for other GTPases, mainly the Ras oncoproteins (29). Rab27a Q78L and Rab3a Q81L are equivalent to Ras Q61L, which has low GTPase activity and stabilizes the GTP-bound, active conformation of the protein. Rab27a T23N corresponds to Ras S17N, which displays lower affinity for GTP than for GDP and exists predominantly in the GDP-bound, inactive conformation. Binding of wild-type Rab27a and Rab27a Q78L to granuphilin, as measured by β-Gal activation, was high, whereas that of Rab27a T23N was much lower (Table 1). Rab3a Q81L also exhibited strong interaction with granuphilin, whereas wild-type Rab3A was inactive. These interactions were specific because neither the C-terminal region containing two C_2 domains of granuphilin nor lamin bound to Rab27a or Rab3a Q81L.

TABLE 1. Quantification of the interaction of granuphilin bait and Rab prey clones[a]

Clone	β-Gal activity (nmoL/min/mg of protein) for vector[b]:		
	pLexGrp.zf	pLexGrp.C_2AB	pLexLamin
pPreyRab27a wt[c]	392	2.0	0.1
pPreyRab27a Q78L	312	0.1	0.2
pPreyRab27a T23N	30	0.1	0.2
pPreyRab3a wt	31	0.5	0.2
pPreyRab3a Q81L	322	0.2	0.3
pVP16	1.5	0.1	0.2

[a] Results were obtained from yeast two-hybrid assays by transactivation of β-Gal activity. Data are given as mean values from two independent experiments, each of which contains triplicate determinations.

[b] pLexGrp.zf and pLexGrp.C_2AB contain the cDNA coding for an N-terminal zinc-finger domain and C-terminal C_2 domains of granuphilin, respectively, whereas pLexLamin contains lamin cDNA.

[c] wt, wild type.

Although Rab effector generally interacts with the GTP-bound form of Rab protein, granuphilin interacted with wild-type Rab27a and Rab27a Q78L similarly in the two-hybrid assay. We investigated biochemically whether the interaction is dependent on the bound guanine nucleotide. For this purpose, GST-fused wild-type Rab27a protein immobilized on glutathione beads was loaded with either GDP or GTPγS, a nonhydrolyzable analogue of GTP, and then incubated with granuphilin that had been translated in vitro in reticulocyte lysates. We found that granuphilin preferentially bound to GTPγS-loaded Rab27a, although a weak interaction with GDP-bound Rab27a was detected (Fig. 1A). These results indicate that granuphilin directly interacts with the GTP-bound form of Rab27a.

To investigate whether these interactions occur in beta cells under physiologic conditions, Rab27a and Rab3a immunoprecipitates from MIN6 cells, a pancreatic beta cell line, were directly examined for the presence of granuphilin. Rab27a immunoprecipitates contained a significant amount of granuphilin, whereas Rab3a/granuphilin complexes were scarcely detectable (Fig. 1B); however, each immunoprecipitate contained a significant amount of corresponding Rab protein (Fig. 1C). These findings indicate that granuphilin forms a stable complex mainly with Rab27a in MIN6 cells, although there was no discernible difference in the strength of interaction with granuphilin between Rab27a Q78L and Rab3a Q81L in the two-hybrid assay (Table 1).

Tissue distribution of Rab27a and Rab3a. The differences, described above, in the quantity of granuphilin complexes formed by Rab27a and Rab3a may result from different localization. To explore this possibility, the tissue and subcellular distributions of Rab27a and Rab3a were investigated. Western blots of tissue extracts showed that Rab27a, detected as a 28-kDa protein, is most abundantly expressed in pancreatic islets among the tissues examined (Fig. 2A, top panel); it is also significantly expressed in MIN6 cells and in pituitary tissue.

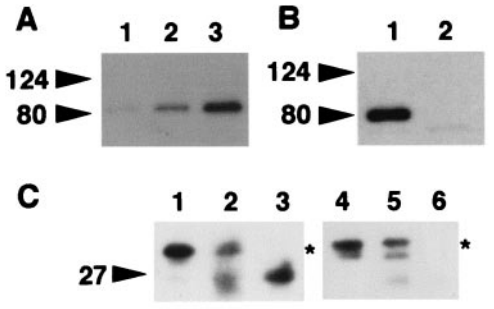

FIG. 1. Complex formation between granuphilin and Rab27a. (A) Guanine nucleotide was exchanged on glutathione beads containing GST-fused wild-type Rab27a in buffer (50 mM Tris-HCl [pH 7.5], 5 mM EDTA, 2 mM $MgCl_2$, 150 mM NaCl, and 0.5 mg of bovine serum albumin/ml) with a 1,000-fold molar excess of either GTPγS or GDP at room temperature for 20 min. After the exchange reaction, $MgCl_2$ was added to a final concentration of 7 mM. Aliquots of beads containing either GST alone (lane 1) or GST-fused Rab27a preloaded with GDP (lane 2) or GTPγS (lane 3) were incubated on ice for 30 min with HA–granuphilin-a that had been translated in vitro using the TNT coupled reticulocyte lysate system (Promega, Madison, Wis.). After washing, granuphilin associated with the beads was detected by immunoblotting using anti-HA antibodies. (B) Extracts of MIN6 cells were incubated with either anti-Rab27a (lane 1) or anti-Rab3a (lane 2) antibodies and then with protein G-Sepharose beads. After the beads were washed, immunoprecipitates were analyzed by immunoblotting using antigranuphilin antibodies (αGrp-aC). Although a Rab3a/granuphilin complex is not visible in this figure, eventually a faint band was observed after longer exposure (data not shown). (C) MIN6 cell extracts (lanes 1 and 4), Rab27a (lane 2) and Rab3a (lane 5) immunoprecipitates as prepared for panel B, and anti-Rab27a (lane 3) and anti-Rab3a (lane 6) antibodies themselves were loaded onto an 18% polyacrylamide gel without dithiothreitol to keep most immunoglobulin G-derived proteins off the 20- to 40-kDa range of gels. Immunoblotting was performed using anti-Rab27a (lanes 1 to 3) and anti-Rab3a (lanes 4 to 6) antibodies. Note that each immunoprecipitate contained a significant amount of corresponding Rab protein (asterisks). Rab3a migrated slower than did a 27-kDa molecular mass marker on nonreducing gels. Numbers to the left of each panel are molecular masses in kilodaltons.

This expression pattern is remarkably similar to that of granuphilin, which is highly and specifically expressed in pancreatic islets and pituitary tissue (37). Longer exposure revealed that Rab27a is weakly but significantly expressed in other tissues such as fat, lung, heart, spleen, and kidney (Fig. 2A, middle panel), whereas it was not detectable in brain, skeletal muscle, liver, testis, or αTC1.6 cells (a pancreatic alpha cell line). On the other hand, Rab3a, detected as a 26-kDa protein, was significantly expressed in brain, pancreatic islets, and MIN6 cells (Fig. 2A, bottom panel). Thus, there is a striking contrast between the expression of Rab27a and that of Rab3a in brain tissue.

Because Rab27a is involved in melanosome transport (1, 19), we examined whether its possible effector, granuphilin, is also expressed in cultured melanocyte cell lines. As expected, Rab27a was significantly expressed in melan-a melanocyte cells and in B16 melanoma cells (Fig. 2B, left panel). Although granuphilin-a (79-kDa protein) and granuphilin-b (59-kDa protein) were significantly expressed in MIN6 cells, neither of them was detectable in these melanocyte cell lines (Fig. 2B, right panel), suggesting that other Rab27a effector proteins act in melanocytes.

Association of Rab27a and Rab3a with dense-core granules. Rab3a associates with synaptic vesicles in neurons and with dense-core granules in endocrine cells (20, 32). The finding that Rab27a is highly expressed in endocrine tissues suggests that Rab27a might be associated with a secretory pathway or organelles enriched in these tissues. We then examined the intracellular distribution of granuphilin, Rab27a, and Rab3a in MIN6 cells by immunofluorescence microscopy. Consistent with our previous finding that granuphilin associates with dense-core granules in MIN6 cells (37), granuphilin showed a punctate pattern similar to that of insulin (Fig. 3A, subpanels a to c). Rab27a also closely resembled the dotted pattern of insulin (Fig. 3A, subpanels d to f) and granuphilin signals (Fig. 3A, subpanels g to i), suggesting that Rab27a associates with dense-core granules. Rab3a also colocalized with insulin and granuphilin (Fig. 3B, subpanels a to d). In addition, granuphilin, Rab27a, and Rab3a were often concentrated just beneath the plasma membrane (Fig. 3A and B).

To substantiate these observations obtained with light microscopy, we then used immunogold electron microscopy of ultrathin frozen sections to examine the localization of these proteins. We found that both granuphilin and Rab27a are indeed localized on the limiting membrane of dense-core gran-

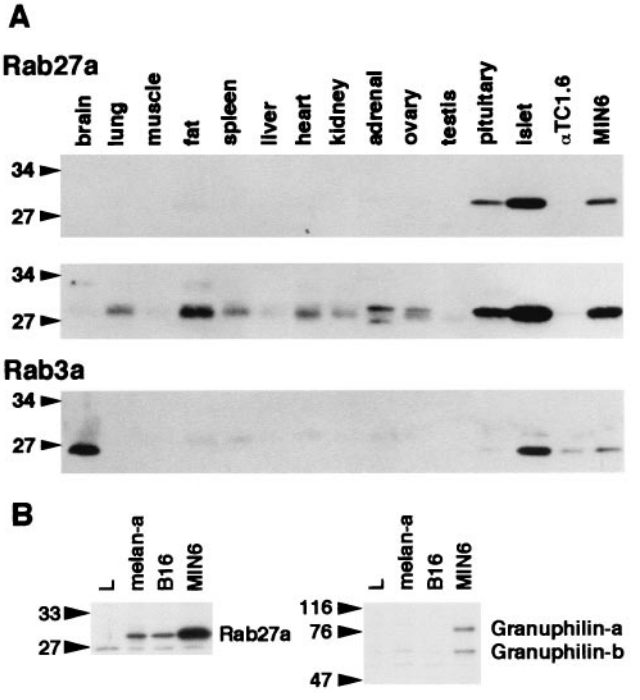

FIG. 2. Tissue and cell expression of Rab27a, Rab3a, and granuphilin. (A) Isolation of mouse pancreatic islets with collagenase and preparation of mouse tissues and cell extracts were performed as described previously (37). An equal amount of protein (100 μg) was loaded onto a polyacrylamide gel. Immunoblotting was performed using anti-Rab27a (top panel) and anti-Rab3a (bottom panel) antibodies. A longer exposure of the Rab27a immunoblot is also shown (middle panel). (B) An equal amount of protein (30 μg) from mouse cell lines (L fibroblast, melan-a melanocyte, B16 melanoma, and MIN6 cells) was loaded onto a polyacrylamide gel. Immunoblotting was performed using anti-Rab27a (left panel) and antigranuphilin (αGrp-N, right panel) antibodies. Numbers to the left of each panel are molecular masses in kilodaltons.

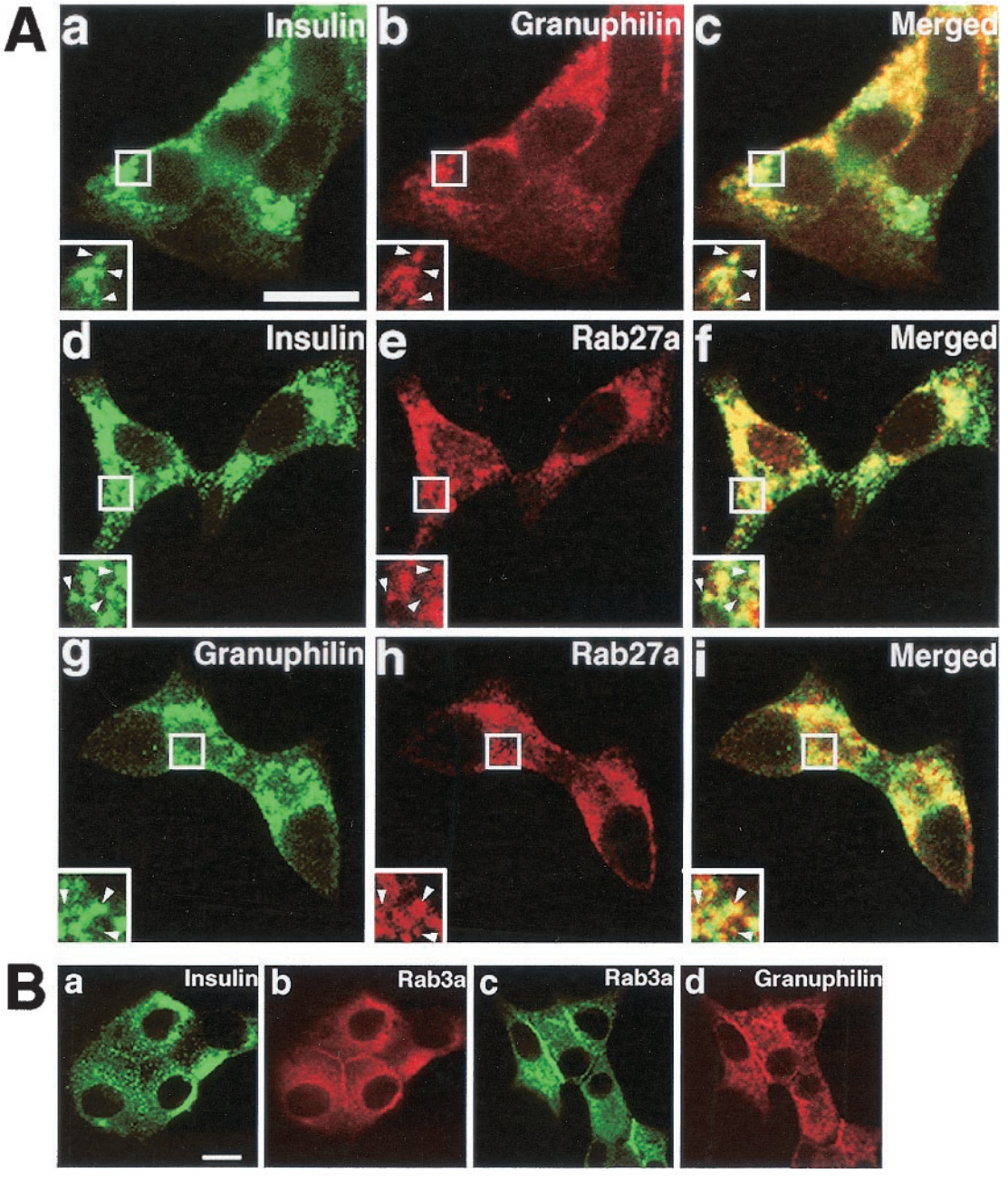

FIG. 3. Intracellular distribution of granuphilin and Rab27a. (A) MIN6 cells were double immunostained with antibodies against insulin (a and d), granuphilin (b and g), and Rab27a (e and h) and examined by confocal microscopy. Merged fluorescent signals are shown in subpanels c, f, and i. Insets represent higher-magnification micrographs of cells within the regions outlined by frames. Images represent single confocal sections. Bar, 10 μm. (B) MIN6 cells were similarly double immunostained with antibodies against insulin, Rab3a, and granuphilin. Bar, 10 μm. (C) Ultrathin cryosections of mouse pancreatic beta cells were immunolabeled with rabbit antibodies against granuphilin (αGrp-N, left panel, 5-nm gold particles) and Rab27a (right panel, 10-nm gold particles). Bar, 500 nm.

ules in pancreatic beta cells (Fig. 3C) and MIN6 cells (data not shown). Granule-associated gold particles as a percentage of all the particles in the cytoplasm of pancreatic beta cells were 53.1% ± 3.8% for granuphilin and 58.4% ± 5.5% for Rab27a, respectively (mean ± standard error of the mean, $n = 10$). Furthermore, we confirmed the previous finding (32) that Rab3a also labeled insulin granules (data not shown). Because the mouse anti-Rab27a and anti-Rab3a antibodies recognized the antigen proteins relatively weakly in the immunogold electron microscopy assay compared with the rabbit antibodies, we could not examine in detail the relative differences in the distribution of these two Rab proteins. Double immunostaining using different sizes of gold particles, however, indicated that at least some granular membrane bears both Rab27a and Rab3a (data not shown).

To further examine the localization of these proteins, we subjected MIN6 cellular membranes to ultracentrifugation in a sucrose gradient under conditions that separate the two types of secretory vesicles in beta cells (31, 37). Insulin-containing dense-core granules and synaptic-like microvesicles that harbor synaptophysin were clearly separated (Fig. 4A, top and bottom panels). Granuphilin immunoreactivity was primarily localized in fractions 8 to 10 (Fig. 4A, second panel from top), which corresponded to the distribution of insulin immunoreactivity. Rab27a exactly colocalized with granuphilin and cosedimented with insulin granules (Fig. 4A, third panel from top). On the other hand, most Rab3a immunoreactivity was localized in a lighter fraction (fraction 2; Fig. 4A, fourth panel from top), although faint Rab3a immunoreactivity was seen in fractions 7 to 10. In contrast to the morphological observation, Rab3a and insulin did not cosediment in the subcellular fractionation analysis. Rab3a might be artificially dissociated from granular membranes during homogenization or subfractionation. To explore this possibility, we examined MIN6 cellular membranes for association of Rab27a and Rab3a (Fig. 4B). Rab27a was found primarily in membrane and detergent-insoluble particulate fractions. In contrast, Rab3a demonstrated roughly equal distribution in the membrane and cytosolic fractions, with none detectable in the particulate fraction. These findings suggest that Rab27a is more tightly associated with membrane than is Rab3a. Although the exact reason for the separation of Rab3a from granule fractions is unknown, it should be noted that granuphilin remained in the fractions containing granules and Rab27a under these experimental conditions (Fig. 4A). These findings support the idea that granuphilin interacts physiologically with Rab27a, but not with Rab3a, in MIN6 cells.

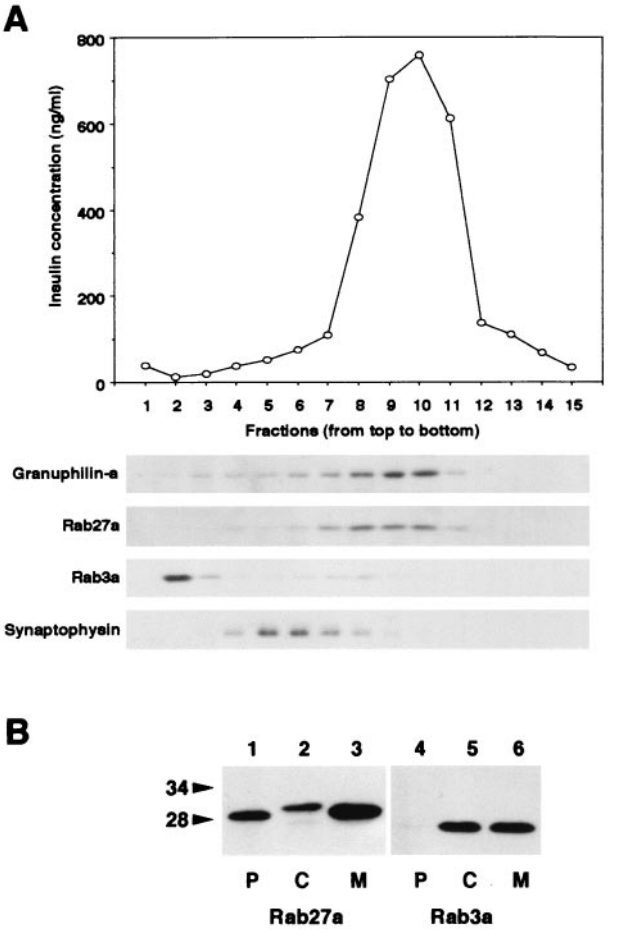

FIG. 4. Subcellular localization of Rab27a and Rab3a. (A) A postnuclear supernatant of MIN6 cells was separated on a linear sucrose density gradient. Fifteen fractions were collected, and immunoreactive insulin in a portion of each fraction was measured (topmost panel). Equal volumes of the fractions were analyzed by immunoblotting using antibodies against granuphilin-a (79-kDa protein), Rab27a (28-kDa protein), Rab3a (26-kDa protein), and synaptophysin (36- to 38-kDa protein). (B) MIN6 cells were fractionated as described previously (5). Briefly, cells were harvested, swollen in hypotonic buffer (20 mM 3-morpholinopropanesulfonic acid [pH 7.3], 1 mM $MgCl_2$, 0.1 mM EDTA, 1 mM phenylmethylsulfonyl fluoride), and ruptured by passage through a 26-gauge needle. After centrifugation at 100,000 × *g* for 60 min, the supernatant (C; soluble cytosolic fraction) was precipitated with 10% trichloroacetic acid plus 0.1% sodium deoxycholate. The pellet was resuspended in hypotonic buffer plus 1% Nonidet P-40. The suspension was centrifuged at 10,000 × *g* for 10 min to separate the supernatant (M; detergent-soluble membrane fraction) and the pellet (P; detergent-insoluble particulate fraction). Equal proportions of the fractions were separated on a polyacrylamide gel for immunoblotting. Numbers to the left of panel B are molecular masses in kilodaltons.

Overexpression of Rab27a enhances insulin secretion. To address the role of Rab27a in the regulated exocytosis of insulin, Rab proteins tagged with the Xpress epitope were transiently overexpressed by using recombinant adenoviruses in MIN6 cells. In addition to the mutants described above, Rab3a T36N, corresponding to Rab27a T23N, which displays lower affinity for GTP than for GDP, and Rab27a N133I and Rab3a N135I, equivalent to Ras N116I, which shows low affinity for both GTP and GDP, were constructed (29). Each form of Rab27a and Rab3a was much more abundantly expressed than were the endogenous proteins as shown by immunoblotting with anti-Rab27a and anti-Rab3a antibodies (Fig. 5, top panels) and was expressed at an equivalent level as revealed by immunoblotting with anti-Xpress antibodies (Fig. 5, middle panel), except for Rab27a T23N and N133I. These two mutants were extremely difficult to express even when a higher titer of recombinant adenovirus was used. Immunostaining with anti-Xpress antibodies indicated that wild-type Rab27a and Rab27a Q78L localize to peripheral granules or along the plasma membrane, whereas Rab27a T23N and N133I are diffusely distributed in the cytoplasm (data not shown), consistent with the expected nature of each form of Rab27a. The immu-

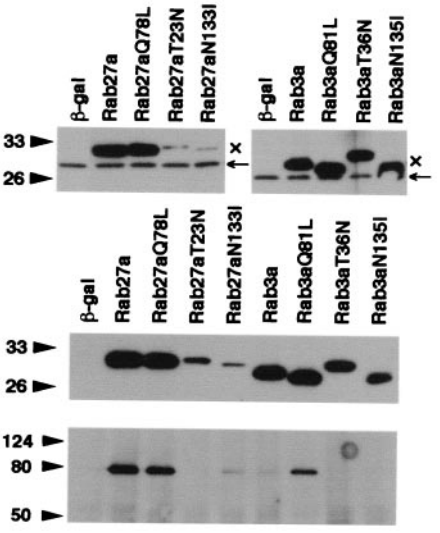

FIG. 5. Overexpression of Rab27a and Rab3a by recombinant adenoviruses. MIN6 cells were infected 40 h before experiments with recombinant adenovirus bearing either β-Gal, Rab27a, or Rab3a cDNA. The expression levels of endogenous (←) and exogenous (×) Rab proteins were determined by immunoblotting with anti-Rab27a (upper left panel) and anti-Rab3a (upper right panel) antibodies. Note that exogenous Rab proteins migrate slower due to the Xpress tag. The expression levels of exogenous Rab27a and Rab3a were compared by immunoblotting with anti-Xpress antibodies (middle panel). Note that each form of Rab27a and Rab3a was expressed at a similar level except for Rab27a T23N and N113I. These two mutants were extremely difficult to express even by using higher PFU per cell. Granuphilin-a associated with each Rab protein was determined by immunoblotting the anti-Xpress immunoprecipitates with antigranuphilin antibodies (αGrp-aC, bottom panel). Numbers to the left of the panels are molecular masses in kilodaltons.

noprecipitates of anti-Xpress antibodies from cells expressing wild-type Rab27a, Rab27a Q78L, and Rab3a Q81L contained significant amounts of endogenous granuphilin, whereas those from cells expressing Rab27a T23N, wild-type Rab3a, and Rab3a T36N and N135I did not (Fig. 5, bottom panel). Rab27a N133I showed a weak interaction with granuphilin. These findings are consistent with the results of the liquid β-Gal assay in the two-hybrid system (Table 1).

The effect of overexpression of these Rab proteins on insulin secretion was next examined (Fig. 6A). High K^+-induced depolarization evokes Ca^{2+}-dependent insulin release in pancreatic beta cells. When 60 mM KCl was applied for 30 min, this relatively strong depolarization condition caused a ninefold increase of insulin release in MIN6 cells (data not shown). Infection with recombinant adenovirus expressing β-Gal did not affect either basal or high K^+-stimulated insulin release. Furthermore, overexpression of any forms of Rab27a or Rab3a did not significantly affect basal insulin secretion. High K^+, however, induced approximately a 15-fold increase in insulin secretion in MIN6 cells overexpressing either wild-type Rab27a or Rab27a Q78L. Thus, depolarization-induced insulin release was enhanced by 50 to 60% in these cells compared with that in uninfected MIN6 cells or those expressing β-Gal. This effect is specific because the enhancement of insulin secretion was dependent on the expression levels of exogenous Rab27a proteins (Fig. 6B). On the other hand, overexpression of Rab27a T23N, Rab27a N133I, wild-type Rab3a, or Rab3a Q81L had no significant effect on high K^+-induced insulin secretion, although the effect of the former two Rab27a mutants could not be properly assessed because of the weak expression. Rab3a Q81L did not show a significant effect on insulin secretion despite the formation of a complex with granuphilin, suggesting that the Rab3a/granuphilin complex does not properly function in MIN6 cells. In contrast, both Rab3a T36N and N135I significantly increased high K^+-induced insulin secretion (about a 30% increase). We also found that overexpression of the N-terminal domain containing a Rab-binding region of granuphilin inhibits insulin secretion (S. Torii and T. Izumi, unpublished data). These findings suggest that Rab27a positively regulates stimulus-induced insulin secretion and that Rab27a and Rab3a have distinct roles in this process.

DISCUSSION

In the present study, we show that Rab27a is highly and specifically expressed in pancreatic islets and pituitary tissues, that Rab27a is localized on the membrane of insulin granules, and that overexpression of Rab27a causes enhancement of high K^+-induced insulin secretion. We also demonstrate that Rab27a interacts with granuphilin, a recently identified rabphilin3-like protein associated with insulin granules (37). The present study describes unexpected findings concerning the Rab proteins involved in the exocytosis of dense-core granules in endocrine cells. Most studies concerning this process have focused on Rab3 (18, 32), based on numerous genetic and biochemical data in neurons. On the other hand, mutations in the Rab27a gene have recently been discovered in patients with Griscelli syndrome (25) and in *ashen* mice (38). Griscelli syndrome is a rare autosomal recessive disorder characterized by pigmentary dilution and immunodeficiency. The *ashen* mutation manifests itself as a lightened coat color and increased bleeding time. These patients and mice exhibit an abnormal accumulation of melanosomes in melanocytes, deficient release of lytic granule content from cytotoxic T lymphocytes, and a reduction in the number of platelet dense granules. Thus, Rab27a appears to play a critical role in the intracellular transport of these organelles. Nevertheless, the data presented here strongly suggest a possible function for the Rab27a GTPase in regulating the exocytosis of dense-core granules in classical endocrine cells such as pancreatic beta cells.

Both Rab27a and Rab3a have an ability to interact with granuphilin, because their active mutants, Rab27a Q78L and Rab3a Q81L, formed a complex with granuphilin to a similar degree in yeast nuclei and in MIN6 cells when overexpressed. We, however, favor Rab27a as a physiological partner of granuphilin in intact cells for the following reasons. First, endogenous Rab27a, but not Rab3a, significantly forms a complex with granuphilin in MIN6 cells. Second, immunoblotting of sucrose gradient fractions reveals that granuphilin remains associated with the granular membrane and cofractionated with Rab27a under conditions where Rab3a appears to be dissociated from the membrane. Finally, the tissue distributions of granuphilin and Rab27a are remarkably similar. Both proteins are highly and specifically expressed in pancreatic islets and in pituitary tissue. Rat Rab27a was previously re-

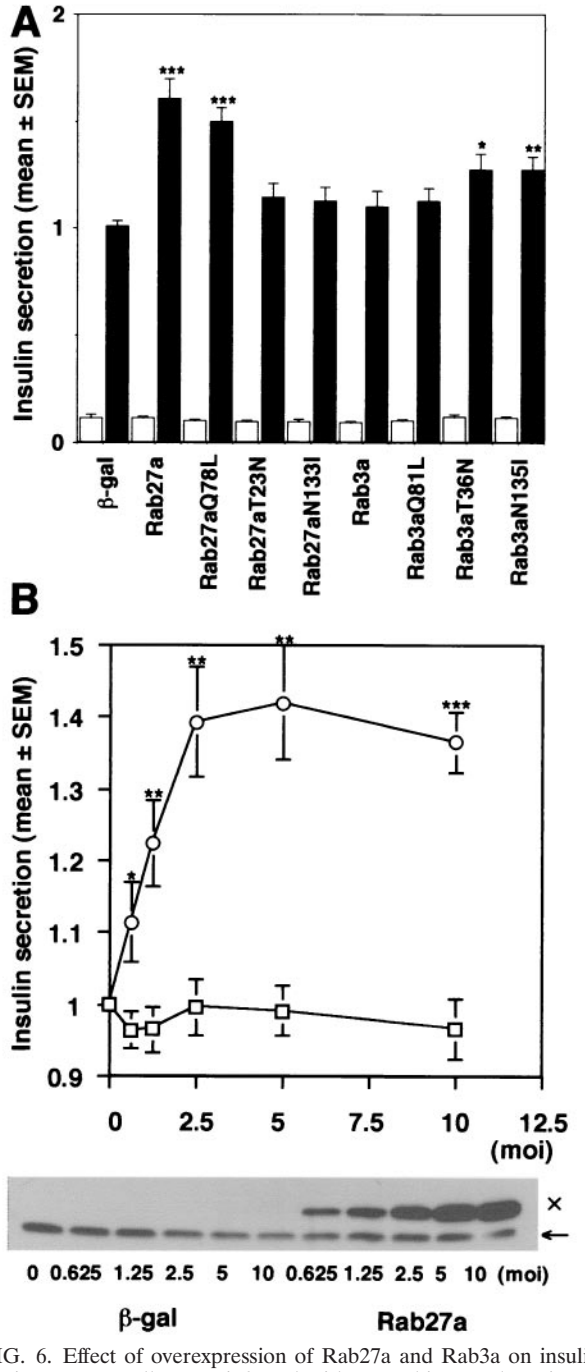

FIG. 6. Effect of overexpression of Rab27a and Rab3a on insulin secretion. MIN6 cells were infected with recombinant adenoviruses bearing either β-Gal or Rab27a cDNA. Insulin in the medium was measured in duplicate. Values were normalized to the release of insulin from uninfected MIN6 cells stimulated by high K^+. The results are given as means ± standard errors of the means (SEMs) of six (A) and five (B) independent experiments. *, $P < 0.05$; **, $P < 0.005$; and ***, $P < 0.0005$, versus high K^+-stimulated MIN6 cells infected with the same titer of the virus bearing β-Gal cDNA. (A) MIN6 cells were infected with recombinant adenoviruses under the same conditions as for Fig. 5. The cells were incubated for 30 min in either modified Krebs-Ringer buffer (open bars) or the buffer modified to include high K^+ (solid bars). (B) MIN6 cells were infected with adenoviruses bearing β-Gal (□) or wild-type Rab27a cDNA (○) at different titers (multiplicity of infection, 0.625 to 10). The cells were incubated for 30 min in modified Krebs-Ringer buffer containing high K^+. The expression levels of Rab27a were shown by immunoblotting with anti-Rab27a antibodies. Note that the expression levels of Rab27a with the Xpress tag (×) increased depending on the virus titer, in contrast to the constant levels of endogenous Rab27a (←).

ported to be ubiquitously expressed in tissues such as spleen, eye, intestine, lung, and pancreas (28, 33). We found that mouse Rab27a is also expressed in some of these tissues, but at relatively low levels. Although its expression in pituitary tissue has been detected by immunohistochemistry (27), previous studies overlooked the highest expression of Rab27a in minor endocrine tissues, due to failure to include these tissues in the analyses. Furthermore, neither Rab27a nor granuphilin is expressed in the brain, where Rab3a and rabphilin3 are abundantly and specifically expressed. It is also notable that rabphilin3 is not expressed in pancreatic islets (32). Thus, the present study demonstrates the correlated expression of two putative sets of Rab bound to its effector protein, Rab27a/granuphilin and Rab3a/rabphilin3. Granuphilin is the first effector protein of Rab27a identified to date. It should be noted, however, that Rab27a, but not granuphilin, is expressed in melanocyte cell lines. Although Rab27a likely functions with granuphilin at least in endocrine cells, it is possible that other effector proteins exist and mediate Rab27a function.

By immunogold electron microscopy, we demonstrated that both Rab27a and Rab3a are localized on the limiting membrane of insulin-containing dense-core granules in pancreatic beta cells. Despite the highest similarity in primary sequence between Rab27 and Rab3 isoforms among Rab proteins, these two Rab proteins appear to have different roles in the exocytotic pathway. We showed that overexpression of wild-type Rab27a or Rab27a Q78L enhances high K^+-induced insulin secretion in MIN6 cells, whereas the comparable expression of wild-type Rab3a or Rab3a Q81L fails to increase it. Because the amount of exocytosis induced by prolonged high K^+ stimulation is considered to represent the size of the pool of fusion-ready vesicles, the simplest interpretation of this finding is that Rab27a acts to maintain the size of this pool by recruiting granules to the docking site. Consistent with this idea, the cells derived from Griscelli syndrome patients or *ashen* mice show that Rab27a is required for the peripheral distribution of melanosomes in melanocytes (1) and for the tight clustering of lytic granules at the immunological synapse in cytotoxic T lymphocytes (35). Genetic and biochemical interaction between Rab27a and the actin-based molecular motor myosin-V also implies that Rab27a is involved in the tethering-docking step before SNARE complex assembly (19, 25). On the other hand, the size and refilling rate of the readily releasable pool are unchanged in Rab3a-deficient synapses (11), suggesting that Rab3a is not involved in trafficking of synaptic vesicles before SNARE complex assembly (20). Instead, enhancement of calcium-triggered fusion and lack of mossy fiber long-term potentiation in these synapses (6, 11, 23) indicate that Rab3a has a role after core complex assembly from SNAREs (20). Defects in exocytosis of secretory granules in endocrine cells, however, have not been reported for either *ashen* mice (38) or Rab3a-knockout mice (11). It is also unclear at present whether Griscelli syndrome patients develop endocrine disorders, as the disease has a poor prognosis and patients do not survive past

childhood (13). Previous studies involving the overexpression of Rab3a in endocrine cells suggest an inhibitory role for Rab3a in exocytosis. For example, overexpression of either Rab3a wild type or Rab3a Q81L inhibits exocytosis in adrenal chromaffin cells (18). Although we could not reproduce the effect of overexpressed wild-type Rab3a or Rab3a Q81L in MIN6 cells, we instead found that inactive Rab3a mutants, Rab3a T36N and N135I, significantly increase high K^+-induced insulin secretion. Thus, Rab27a and Rab3a appear to have opposite effects on stimulus-induced insulin secretion. Further studies are required, however, to clarify the differential and/or redundant roles of Rab27a and Rab3a in the exocytosis of dense-core granules in endocrine cells.

Our biochemical analysis showed that the proportion of Rab27a molecules that are associated with membrane is much higher than that for Rab3a. In addition, a significant fraction of Rab27a was not easily extracted from membrane even after treatment with detergent. Furthermore, we found that Rab27a T23N and N133I, mutants that are presumably not associated with membrane, are extremely refractory to overexpression in intact cells. The unstable nature of these mutants is specific to Rab27a because the equivalent Rab3a mutants, Rab3a T36N and N135I, were easily expressed. These findings suggest that Rab27a is normally associated with membrane and is very unstable when it is not associated with it. This may explain why the Rab27a/granuphilin complex is easily detectable in cells in spite of the transitory nature of GTPase target interactions. Furthermore, it may explain why the function of Rab27a is particularly sensitive to general defects in lipidation and membrane association of Rab proteins. Rab27a has been implicated in two other disease states. One is choroideremia, the X-linked human retinal degenerative disease, which is caused by mutation of Rab escort protein-1 (33). Another is the *gunmetal* mouse, whose coat color dilution and dysfunction of platelet granules are caused by mutation of Rab geranylgeranyl transferase α (10). Although these mutations should impair lipidation and membrane association of any Rab protein, they apparently lead to hypoprenylation-dysfunction of selected members of the Rab protein family such as Rab27a.

It has recently been demonstrated that Rab27a associates with melanosomes in melanocytes (1, 19) and lytic granules in cytotoxic T lymphocytes (14). For the storage and release of their secretory products, these cells use special organelles, termed secretory lysosomes, that show mixed features of lysosomes and secretory granules on many different levels (34). Although the morphological features and the biogenesis of granules and lysosomes are quite different, it has been shown elsewhere that newly synthesized lysosomal proteins enter immature granules and are sorted out later in pancreatic beta and acinar cells (21, 22). Thus, the immature granules may be considered a post-Golgi intermediate on the pathway to these distinct organelles. It is possible that other key proteins, such as Rab effectors and SNAREs, are also shared between these two organelles.

In summary, we present evidence that Rab27a and its effector protein, granuphilin, are involved in the exocytosis of dense-core granules in endocrine cells, although the precise function of this complex remains unknown. The present study also provides the unexpected finding that Rab27a is commonly used in the exocytotic pathways of conventional secretory granules and secretory lysosomes. Furthermore, our study may be the first to provide evidence that the exocytosis of synaptic vesicles in neurons and of dense-core granules in endocrine cells is regulated by different sets of Rab and effector proteins. Identification of the Rab27a/granuphilin complex will facilitate clarification of common and different aspects of the exocytotic machinery in these secretory cells.

ACKNOWLEDGMENTS

This work was supported by a grant-in-aid for scientific research from the Ministry of Education, Science, Sports, and Culture of Japan. It was also supported in part by the Ministry of Health and Welfare of Japan (Research on Human Genome and Gene Therapy) and by grants from the Japan Diabetes Foundation, the Suzuken Memorial Foundation, and the Japan Insulin Study Group Award, to T.I.

We thank S. M. Hollenberg (Vollum Institute, Oregon Health Sciences University) for providing reagents of the yeast two-hybrid system and H. Fujita (Kyushu University) for providing melanocyte cell lines. We also thank E. Erikson (University of Colorado School of Medicine) for critical reading of the manuscript and H. Tamemoto, S. Mizutani, J. Wang, and K. Nagashima (Institute for Molecular and Cellular Regulation, Gunma University) for generous support and useful advice.

REFERENCES

1. **Bahadoran, P., E. Aberdam, F. Mantoux, R. Buscà, K. Bille, N. Yalman, G. de Saint-Basile, R. Casaroli-Marano, J.-P. Ortonne, and R. Ballotti.** 2001. Rab27a: a key to melanosome transport in human melanocytes. J. Cell Biol. **152:**843–849.
2. **Bartel, P. L., and S. Fields.** 1995. Analyzing protein-protein interactions using two-hybrid system. Methods Enzymol. **254:**241–263.
3. **Baumart, M., G. Fischer von Mollard, R. Jahn, and T. C. Südhof.** 1993. Structure of the murine *rab3A* gene: correlation of genomic organization with antibody epitopes. Biochem. J. **293:**157–163.
4. **Bock, J. B., H. T. Matern, A. A. Peden, and R. H. Scheller.** 2001. A genomic perspective on membrane compartment organization. Nature **409:**839–841.
5. **Brondyk, W. H., C. J. McKiernan, K. A. Fortner, P. Stabila, R. W. Holz, and I. G. Macara.** 1995. Interaction cloning of Rabin3, a novel protein that associates with the Ras-like GTPase Rab3A. Mol. Cell. Biol. **15:**1137–1143.
6. **Castillo, P. E., R. Janz, T. C. Südhof, T. Tzounopoulos, R. C. Melanke, and R. A. Nicoll.** 1997. Rab3A is essential for mossy fibre long-term potentiation in the hippocampus. Nature **388:**590–593.
7. **Chen, D., J. Guo, T. Miki, M. Tachibana, and W. A. Gahl.** 1997. Molecular cloning and characterization of rab27a and rab27b, novel human rab proteins shared by melanocytes and platelets. Biochem. Mol. Med. **60:**27–37.
8. **Coombs, D. H.** 1975. Density gradient fractionation by piston displacement. Anal. Biochem. **68:**95–101.
9. **Coombs, D. H., and N. R. M. Watts.** 1985. Generating sucrose gradients in three minutes by tilted tube rotation. Anal. Biochem. **148:**254–259.
10. **Detter, J. C., Q. Zhang, E. H. Mules, E. K. Novak, V. S. Mishra, W. Li, E. B. McMurtrie, V. T. Tchernev, M. R. Wallace, M. C. Seabra, R. T. Swank, and S. F. Kingsmore.** 2000. Rab geranylgeranyl transferase α mutation in the *gunmetal* mouse reduces Rab prenylation and platelet synthesis. Proc. Natl. Acad. Sci. USA **97:**4144–4149.
11. **Geppert, M., Y. Goda, C. F. Stevens, and T. C. Südhof.** 1997. The small GTP-binding protein Rab3A regulates a late step in synaptic vesicle fusion. Nature **387:**810–814.
12. **Griffith, G., A. McDowall, R. Back, and J. Dubochet.** 1984. On the preparation of cryosections for immunocytochemistry. J. Ultrastruct. Res. **89:**65–78.
13. **Griscelli, C., A. Durandy, D. Guy-Grand, F. Daguillard, C. Herzog, and M. Prunieras.** 1978. A syndrome associating partial albinism and immunodeficiency. Am. J. Med. **65:**691–702.
14. **Haddad, E. K., X. Wu, J. A. Hammer III, and P. A. Henkart.** 2001. Defective granule exocytosis in Rab27a-deficient lymphocytes from *Ashen* mice. J. Cell Biol. **152:**835–841.
15. **Hirayama, I., H. Tamemoto, H. Yokota, S.-K. Kubo, J. Wang, H. Kuwano, Y. Nagamachi, T. Takeuchi, and T. Izumi.** 1999. Insulin receptor-related receptor is expressed in pancreatic β-cells and stimulates tyrosine phosphorylation of insulin receptor substrate-1 and -2. Diabetes **48:**1237–1244.
16. **Hoffman, C. S., and F. Winston.** 1987. A ten-minute DNA preparation from yeast efficiently releases autonomous plasmids for transformation of *Escherichia coli*. Gene **57:**267–272.
17. **Hollenberg, S. M., R. Sternglanz, P. F. Cheng, and H. Weintraub.** 1995. Identification of a new family of tissue-specific basic helix-loop-helix proteins with a two-hybrid system. Mol. Cell. Biol. **15:**3813–3822.
18. **Holz, R. W., W. H. Brondyk, R. A. Senter, L. Kuizon, and I. G. Macara.** 1994.

Evidence for the involvement of Rab3A in Ca^{2+}-dependent exocytosis from adrenal chromaffin cells. J. Biol. Chem. **269:**10229–10234.
19. **Hume, A. N., L. M. Collinson, A. Repak, A. Q. Gomes, C. R. Hopkins, and M. C. Seabra.** 2001. Rab27a regulates the peripheral distribution of melanosomes in melanocytes. J. Cell Biol. **152:**795–808.
20. **Jahn, R., and T. C. Südhof.** 1999. Membrane fusion and exocytosis. Annu. Rev. Biochem. **68:**863–911.
21. **Klumperman, J., R. Kuliawat, J. M. Griffith, H. J. Geuze, and P. Arvan.** 1998. Mannose 6-phosphate receptors are sorted from immature secretory granules via adaptor protein AP-1, clathrin, and syntaxin 6-positive vesicles. J. Cell Biol. **141:**359–371.
22. **Kuliawat, R., J. Klumperman, T. Ludwig, and P. Arvan.** 1997. Differential sorting of lysosomal enzymes out of the regulated secretory pathway in pancreatic β-cells. J. Cell Biol. **137:**595–608.
23. **Lonart, G., R. Janz, K. M. Johnson, and T. C. Südhof.** 1998. Mechanism of action of rab3A in mossy fiber LTP. Neuron **21:**1141–1150.
24. **McBride, H. M., V. Rybin, C. Murphy, A. Giner, R. Teasdale, and M. Zerial.** 1999. Oligomeric complexes link Rab5 effectors with NSF and drive membrane fusion via interactions between EEA1 and syntaxin 13. Cell **98:**377–386.
25. **Ménasché, G., E. Pastural, J. Feldmann, S. Certain, F. Ersoy, S. Dupuis, N. Wulffraat, D. Bianchi, A. Fischer, F. Le Deist, and G. de Saint Basile.** 2000. Mutations in *RAB27A* cause Griscelli syndrome associated with haemophagocytic syndrome. Nat. Genet. **25:**173–176.
26. **Miyake, S., M. Makimura, Y. Kanegae, S. Harada, Y. Sato, K. Takamori, C. Tokuda, and I. Saito.** 1996. Efficient generation of recombinant adenoviruses using adenovirus DNA-terminal protein complex and a cosmid bearing the full-length virus genome. Proc. Natl. Acad. Sci. USA **93:**1320–1324.
27. **Nagata, K., H. Sakagami, H. Kondo, and Y. Nozawa.** 1995. Identification and localization of gene expression of a low Mr GTP-binding protein, *ram* p25 in pituitary gland. Biochem. Biophys. Res. Commun. **217:**1223–1230.
28. **Nagata, K., T. Satoh, H. Itoh, T. Kozasa, Y. Okano, T. Doi, Y. Kaziro, and Y. Nozawa.** 1990. The *ram*: a novel low molecular weight GTP-binding protein cDNA from a rat megakaryocyte library. FEBS Lett. **275:**29–32.
29. **Olkkonen, V. M., and H. Stenmark.** 1997. Role of Rab GTPases in membrane traffic. Int. Rev. Cytol. **176:**1–85.
30. **Pfeffer, S. R.** 1999. Transport-vesicle targeting: tethers before SNAREs. Nat. Cell Biol. **1:**E17-E22.
31. **Reetz, A., M. Solimena, M. Matteoli, F. Folli, K. Takei, and P. De Camilli.** 1991. GABA and pancreatic β-cells: colocalization of glutamic acid decarboxylase (GAD) and GABA with synaptic-like microvesicles suggests their role in GABA storage and secretion. EMBO J. **10:**1275–1284.
32. **Regazzi, R., M. Ravazzola, M. Iezzi, J. Lang, A. Zahraoui, E. Andereggen, P. Morel, Y. Takai, and C. B. Wollheim.** 1996. Expression, localization and functional role of small GTPases of the Rab3 family in insulin-secreting cells. J. Cell Sci. **109:**2265–2273.
33. **Seabra, M. C., Y. K. Ho, and J. S. Anant.** 1995. Deficient geranylgeranylation of ram/rab27 in choroideremia. J. Biol. Chem. **270:**24420–24427.
34. **Stinchcombe, J. C., and G. M. Griffiths.** 1999. Regulated secretion from hemopoietic cells. J. Cell Biol. **147:**1–5.
35. **Stinchcombe, J. C., D. C. Barral, E. H. Mules, S. Booth, A. N. Hume, L. M. Machesky, M. C. Seabra, and G. M. Griffiths.** 2001. Rab27A is required for regulated secretion in cytotoxic T lymphocytes. J. Cell Biol. **152:**825–833.
36. **Torii, S., D. A. Egan, R. A. Evans, and J. C. Reed.** 1999. Human Daxx regulates Fas-induced apoptosis from nuclear PML oncogenic domains (PODs). EMBO J. **18:**6037–6049.
37. **Wang, J., T. Takeuchi, H. Yokota, and T. Izumi.** 1999. Novel rabphilin3-like protein associates with insulin-containing granules in pancreatic beta cells. J. Biol. Chem. **274:**28542–28548.
38. **Wilson, S. M., R. Yip, D. A. Swing, T. N. O'Sullivan, Y. Zhang, E. K. Novak, R. T. Swank, L. B. Russell, N. G. Copeland, and N. A. Jenkins.** 2000. A mutation in *Rab27A* causes the vesicle transport defects observed in *ashen* mice. Proc. Natl. Acad. Sci. USA **97:**7933–7938.